Conformational Aspects of Poly(vinyl acetate)

P. R. Sundararajan

Xerox Research Centre of Canada Limited, Mississauga, Ontario L5L 1J9, Canada.
Received September 29, 1977

ABSTRACT: Conformational features of meso and racemic dyads of poly(vinyl acetate) (PVAc) are examined using energy calculations. In contrast to other vinyl chains bearing planar substituent, the $\bar{g}$ conformation is not prohibited for this polymer. The extended chain conformation (ttt . . .) is comparable in energy to the helical conformations (tgtg . . .) for isotactic PVAc. The shifts in the positions of the energy minima from perfect staggering are discussed in terms of the second-order interactions. Calculated statistical weight parameters are used to reproduce the experimental data on NMR coupling constants and the characteristic ratios.

Energy calculations using semiempirical methods have in the past been applied to evaluate the conformational characteristics of mono- and disubstituted vinyl chains.[1-6] The work on polystyrene[2] (PS), poly(methyl acrylate)[3] (PMA), poly(methyl methacrylate)[4,5] (PMMA), and poly(α-methylstyrene)[6] (PMS) showed that (i) the overlap between the substituents which occur in the tt state of the meso dyad can be relieved appreciably by a slight variation of the rotation about the skeletal bonds so that the population of this state becomes significant and (ii) in all these cases, the $\bar{g}$ conformation of the skeletal bonds is ruled out. The severe overlap between the atoms which preclude the $\bar{g}$ conformation is necessarily due to the planarity of the side group in these polymers.

The conformational features of poly(vinyl acetate) (PVAc) are presented here. This monosubstituted chain contains a planar side group which differs from PMA and PS in that the C^β atom is replaced by the oxygen and the configuration, or the disposition, of the bonds linked to the oxygen atom is different from that of the bonds linked to the C^β atom in PMA and PS. It would be of interest to see if the elimination of $\bar{g}$ conformation is valid for this polymer as well.

Poly(vinyl acetate) is one of the very few polymers which can be synthesized to be exactly atactic.[7,8] It is commonly assumed, although erroneously, that all non-crystallizable polymers are atactic. The NMR results of Bovey showed that the conventional "atactic" polymers are indeed predominantly syndiotactic.[7]

Poly(vinyl acetate) can be prepared with any tacticity, ranging from 90% isotactic to 75% syndiotactic. Poly(vinyl alcohol) (PVA) and PVAc are interconvertible without isomerization. Although PVA of any tacticity can be crystallized, all attempts to crystallize PVAc, even in the highest isotactic form, have been unsuccessful.[8]

The conformational characteristics of a monosubstituted chain can, in general, be assessed on the basis of interactions of second order.[1-3,9,10] Such interactions involve atoms or groups separated by four bonds (two skeletal and two pendant) and hence these are also known as four-bond interactions. The distance between the centers of two groups thus related depends on the angles of rotation about the central pair (skeletal) of the sequence of four bonds. Although the intensity of the interaction depends also on the rotations about the two outer or pendant bonds of the sequence, these rotations can generally be neglected. Thus, the identities of the individual atoms of a group are omitted for the purpose of formulation of the problem. Variation in the interaction if any, due to the side group rotation mentioned above, is implicit and is considered collectively as the second-order interaction. Higher order interactions, i.e., overlaps caused by rotations around three or more skeletal bonds, involve the $g\bar{g}$ or $\bar{g}g$ state of a pair of contiguous skeletal bonds. The $g\bar{g}$ and $\bar{g}g$ states are of extremely low incidence due to the severity of second-order interactions in these conformations. The exclusion of the above states on the basis of second-order interactions obviates the need to consider interactions of higher order. Thus, the problem reduces to the formulation of statistical weight matrices[9,10] embracing (i) the bond pair flanking the C^α atom (U'), (ii) the bonds between two successive C^α atoms in a meso dyad (U''_m), and (iii) such a bond pair in a racemic dyad (U''_r). These are given by

$$\mathbf{U}' = \begin{bmatrix} \eta & 1 & \tau \\ \eta & 0 & \tau \\ \eta & 1 & 0 \end{bmatrix} \tag{1}$$

$$\mathbf{U}''_m = \begin{bmatrix} \eta\omega'' & 1 & \tau\omega' \\ \eta & \omega & \tau\omega' \\ \eta\omega' & \omega' & \tau\omega\omega'' \end{bmatrix} \tag{2}$$

and

$$\mathbf{U}''_r = \begin{bmatrix} \eta & \omega' & \tau\omega'' \\ \eta\omega' & 1 & \tau\omega \\ \eta\omega'' & \omega & \tau\omega'^2 \end{bmatrix} \tag{3}$$

The parameters η and τ pertain to the first-order interactions in the t and $\bar{g}$ states. The second-order interactions involving the pairs $CH_2 \cdots CH_2$, $CH_2 \cdots R$, and $R \cdots R$ are represented by ω, ω', and ω'', respectively.

Energy Calculations

A segment of isotactic PVAc is shown in Figure 1a, with all the skeletal bonds in the trans conformation, which defines $\phi_i = 0$. The designations of the bonds and the rotations are also shown. Following Flory et al.,[10] enantiomeric bonds are defined with respect to the chirality of the bonds. This is accomplished by viewing all the bonds from the C^α atom to the methylene group, without regard to the direction of progression of the chain. While viewing along a bond such as i, if the substituent R is to the right, as in Figure 1b, the bond belongs to the d species. The bond $i + 1$, as shown in Figure 1b, belongs to the l species. A consequence of this definition is that the bonds which flank a C^α atom are of opposite character. An isotactic chain is generated by a sequence of |dl|dl| bonds and the |dd|ll|dd| progression characterizes a syndiotactic chain. The vertical bars denote the location of the C^α atoms. Viewing along the bonds from the C^α atom to the methylene group, a right-handed rotation about the d bond increases the value of ϕ. Likewise, the rotations about the l bonds are left handed.

The bond lengths and bond angles are listed in Table I. The angle C^α–C–C^α was taken to be 114°, as in the cases of PS[2] and PMA.[3] The acetate group was taken to be in the trans planar conformation, with the partial double bond eclipsing the C^α–H

0024-9297/78/2211-0256$01.00/0

Table I
Bond Lengths and Bond Angles Used in This Study

Atoms in bond	Bond length, Å	Atoms in bond	Bond angle, deg
C^{α}–C	1.53	C^{α}—C—C^{α}	114
C^{α}–O	1.42	C—C^{α}—C	109.5
C^{α}–H	1.10	C^{α}—O=C	113
C–O (ester)	1.36	O=C=O	118
C–O (carbonyl)	1.25	O=C—CH_3	122
C–CH_3	1.52	C—C^{α}—O	109.5

Table II
Parameters for Nonbonded Interaction Energy

Atom or group	Polarizability α	Effective no. of electrons	van der Waals radius, Å
C	0.93	5	1.8
C (carbonyl)	1.23	5	1.8
O	0.64	7	1.6
O (carbonyl)	0.84	7	1.6
CH_2 or CH_3	1.77	7	2.0
H	0.42	0.9	1.3

bond. This defines $\chi = 0$. Experimental[11] and theoretical calculations[12–14] on the orientation of the acetate groups in several polymers and analogues show that the carbonyl bond is in the syn-planar conformation with respect to the substituent at the C^{α} atom and that the variation in χ is restricted to ±20°. Hence, $\chi = 0$ was assumed in the calculations which follow.

A threefold intrinsic torsional potential, with a barrier of 2.8 kcal mol^{-1}, was assigned for the two rotations around the skeletal bonds. The Lennard–Jones 6–12 potential functions, with parameters given in Table II, were used for estimating the nonbonded interaction energies.[1–6] Coulombic interactions were calculated using the method of Brant et al.[15] and assigning partial charges to the atoms using bond moments of 0, 0.82, 0.74, 2.3, and 0.38D for C—C, C—O, C=O, C=O, and C—H bonds, respectively.[16] A value of 4.0 was used for the effective dielectric constant.[3–6]

A truncation procedure which was used for PS, PMMA, PMA, and PMS was followed to allow for the conformation dependence of solvent interaction.[2–6] For vinyl chains such as above, with a large and planar side group R, the interaction between R_{i-1} and R_{i+1} is large in conformations such as tt of the meso dyad. The proximity of the R groups in such a conformation prevents access of solvent molecules. In a conformation such as tg or gt of a meso dyad, the interaction between the R groups is negligible but this decrease in interaction is compensated by the interaction between the R group and the solvent molecules since the former is now in a favorable position to interact with the solvent. Thus, beyond a certain distance which is sufficient to permit entry of solvent molecules, the reduced R···R interaction will be replaced by R···solvent interaction. The energy of the system will thus level off at this distance. Following the previous procedure,[2,3,5,6] the calculated energy remains at the value for $r = \sigma$ for all distances greater than σ. Here σ is a suitably chosen truncation distance. Although the exact value of σ is difficult to estimate, previous calculations showed a value of 5 Å for all atom pairs to be reasonable.[2,3] Use of different values for σ changes the relative energies of the conformations but the locations of minima are not affected. This empirical procedure has been successful in reproducing the experimental data on several polymers mentioned before.[2–6,17,18] A similar method was used by Bleha and Valko[19] for PVA in which the value of the statistical weight parameter for OH···OH interaction was

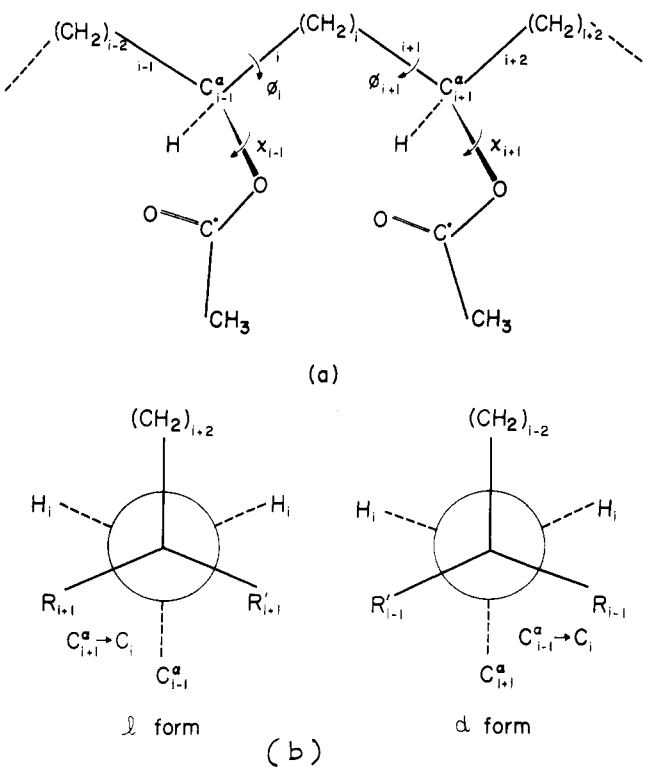

Figure 1. (a) Schematic of a segment of isotactic PVAc. (b) Newman diagrams for the bonds i and $i + 1$ in the trans conformation.

varied to reproduce the characteristic ratio for isotactic PVA in solvents of different polarity, which hydrogen bond to the chain to various extents.

The calculations on PMA showed that the values of the relative energies with $\sigma = \infty$ and $\sigma = 5$ Å were not significantly different. This is contrary to the results on PS and PMS and was attributed to the smaller size of the $COOCH_3$ group compared to the phenyl. In the present case, in addition to the values of ∞ and 5 Å for σ, a value of $r_i + r_j + 0.2$ was also used. Here r_i and r_j are the van der Waals radii of atoms i and j. The use of the sum of the radii imposes a dependence of σ on the pair of atoms which interact. For a pair of methyl groups, the value of σ becomes 4.2 Å, slightly larger than the value of 3.9 Å examined by Yoon et al.[2,3] For the rest of the pairs the value of σ is smaller. The additional factor of 0.2 Å was chosen arbitrarily.

Energy Maps

Conformational energy maps calculated for the meso and racemic dyads of PVAc, with $\sigma = \infty$, are shown in Figures 2 and 3 as a function of the skeletal rotation angles ϕ_i and ϕ_{i+1}. The contours, drawn at intervals of 2 kcal mol^{-1}, are expressed relative to the minimum for the tt state of the racemic dyad. As set forth above, the rotation ϕ_i in Figure 2 is measured in the right-handed sense while ϕ_{i+1} is left handed.

The important feature of the maps in Figures 2 and 3 is that there are well-defined minima corresponding to the $\bar{g}$ state of the bonds i and $i + 1$. It is seen that the meso, $\bar{g}t$ or $t\bar{g}$ state is only 1.1 kcal mol^{-1} higher in energy than the meso, tt state. The racemic, $\bar{g}t$ or $t\bar{g}$ state is 2.1 kcal mol^{-1} higher than the racemic, tt state. Thus the contribution of the $\bar{g}$ state of the bonds is significant.

This result is significantly different from that for all the vinyl chains with planar side groups examined previously. This is due to the presence of the oxygen atom in PVAc in the place of the C^{β} atoms, as shown in Figure 4. Figure 4a shows the "forked" disposition of the bonds about the C^{β} atom, in, e.g., PMA. This results in an overlap between the atom A or

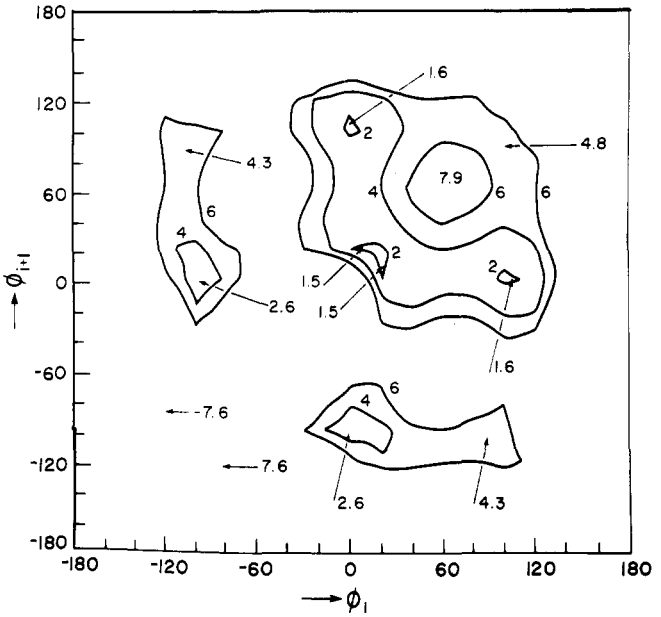

Figure 2. Energy contours in kcal mol^{-1} for the meso dyad. Contours are drawn at intervals of 2 kcal mol^{-1} relative to the minimum in the racemic, tt state.

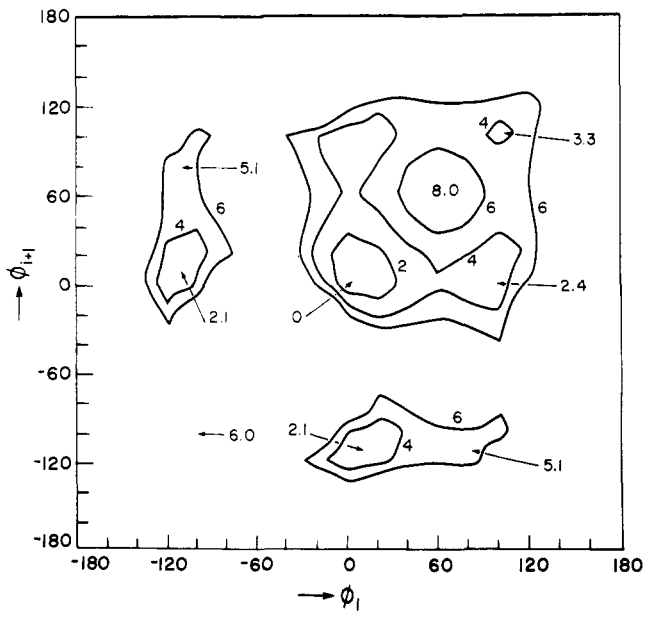

Figure 3. Energy contours, in kcal mol^{-1}, for the racemic dyad.

B attached to C^β and the atoms attached to the next C^α atom. Since either A or B causes overlap, the severity of this overlap is independent of the value of χ. However, in the case of PVAc, as shown in Figure 4b, such a forked disposition does not exist. In fact, the preferred orientation of the acetate group, which renders the O=C bond to eclipse the C^α—H bond, avoids any severe overlap of the atoms of the acetate group with those attached to the next C^α atom. Hence, the $\bar{g}$ state cannot be ruled out as was done for PS, PMS, PMA, and PMMA.

The minima are shifted from the perfect staggering as observed in other cases. The "split" (or doublet of) minima which are characteristic of disubstituted chains do not occur here except for the $\bar{g}\bar{g}$ state of the meso dyad. The minimum for the meso, tt state occurs at $(\phi_i,\phi_{i+1}) = (20°,10°)$ and $(10°,20°)$. For the perfectly staggered position, (0°,0°), the energy is too high. The distances $O_{i-1}\cdots O_{i+1}$, $C^*_{i-1}\cdots C^*_{i+1}$, and

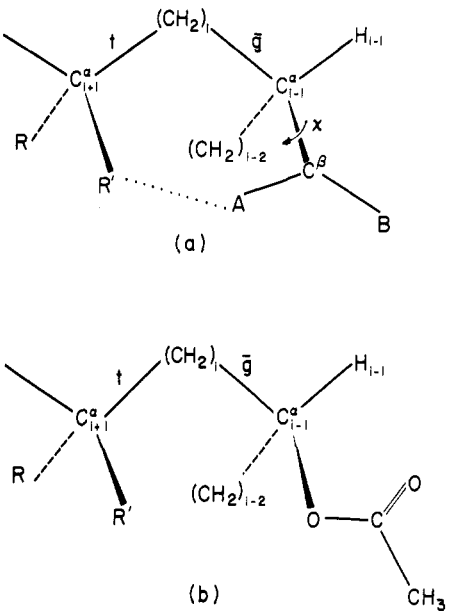

Figure 4. Disposition of side-chain bonds in the $\bar{g}$ conformation of the skeletal bonds. (a) The forked configuration about the C^β atom for PS and PMA. The atoms attached to C^β are denoted as A and B. (b) The $\bar{g}$ conformation in PVAc. Note that in both (a) and (b) the atoms are numbered, for clarity, in opposite direction to that in Figure 1a.

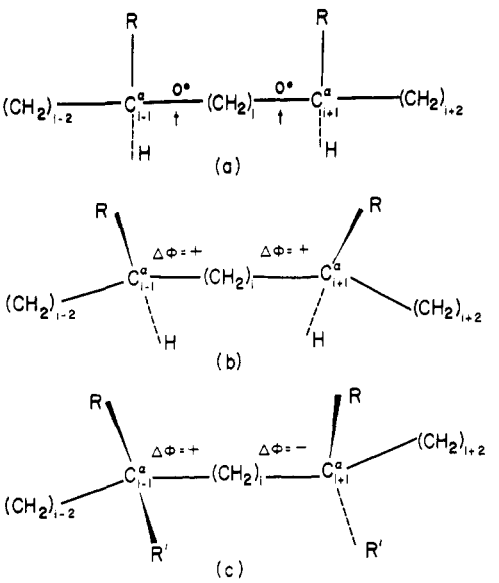

Figure 5. The relative positioning of side-group bonds for different signs of $\Delta\phi$ in the tt state of the meso dyad. (a) Perfectly staggered position with $\Delta\phi = 0$. (b) A (+,+) shift in ϕ_i and ϕ_{i+1} is shown. The R···R distance increases and the H···H distance decreases. This situation is found for PS, PMA, and PVAc. (c) A (+,−) shift in ϕ_i,ϕ_{i+1} which occurs in PMMA and PMS. The distances R···R and R′···R′ are simultaneously increased.

$(CH_3)_{i-1}\cdots(CH_3)_{i+1}$ are 2.63, 2.73, and 2.82 Å, respectively. For (20°,10°), these distances increase to 2.99, 3.07, and 3.51 Å, which reduces the repulsion between these atoms or groups significantly. The shifts $\Delta\phi_i$ and $\Delta\phi_{i+1}$ are both positive, (+,+), for ϕ_i and ϕ_{i+1}. This again contrasts the situation in disubstituted chains such as PMMA and PMS in which these shifts are of opposite signs, i.e., (+,−) or (−,+). The comparison is made in Figure 5, in which the views of the bonds for various displacements in the tt state are shown. Viewing parallel to the plane containing C^α_{i-1} and C^α_{i+1}, as in Figure

Table III
Average Parameters Deduced from Energy Calculations[a]

Parameter	tt	gt	$\bar{g}t$	gg	$g\bar{g}$	$\bar{g}\bar{g}$
			Meso dyad, $\sigma = \infty$			
z	0.16	0.10	0.014	0.001	0.001	0
$\langle E \rangle$	1.4	1.6	2.5	4.5	4.2	7.5
$\langle \phi_i, \phi_{i+1} \rangle$	18,18	102,3	−101,6	96,76	90,−107	−101,−101
			Meso dyad, σ = 5 Å			
z	0.16	0.17	0.02	0.002	0.001	0
$\langle E \rangle$	1.4	1.2	2.2	4.1	4.0	7.5
$\langle \phi_i, \phi_{i+1} \rangle$	19,19	102,3	−101,6	97,81	91,−108	−102,−102
			Meso dyad, $\sigma = r_i + r_j + 0.2$			
z	0.12	0.45	0.04	0.02	0.01	0
$\langle E \rangle$	1.76	0.65	1.86	2.9	2.8	6.6
$\langle \phi_i, \phi_{i+1} \rangle$	21,21	105,3	−104,10	96,84	91,−108	−102,−102
			Racemic dyad, $\sigma = \infty$			
z	1.0	0.03	0.03	0.005	0.001	0
$\langle E \rangle$	0	2.41	2.03	3.36	4.3	5.9
$\langle \phi_i, \phi_{i+1} \rangle$	7,7	94,6	−111,10	103,103	60,−107	−97,−97
			Racemic dyad, σ = 5 Å			
z	1	0.04	0.02	0.01	0.001	0
$\langle E \rangle$	0	2.19	2.17	2.84	4.2	5.4
$\langle \phi_i, \phi_{i+1} \rangle$	7,7	96,8	−111,11	103,103	64,−107	−97,−97
			Racemic dyad, $\sigma = r_i + r_j + 0.2$			
z	1	0.16	0.08	0.07	0.005	0
$\langle E \rangle$	0	1.33	1.4	1.72	3.3	5.0
$\langle \phi_i, \phi_{i+1} \rangle$	8,8	96,8	−113,10	104,104	72,−108	−98,−98

[a] The values of z and E are expressed relative to the racemic, tt state. The values of tg, t$\bar{g}$, and $\bar{g}$g are the same as for gt, $\bar{g}$t, and g$\bar{g}$ states, respectively.

5a, the side-chain bonds attached to the C^{α} atoms are vertically below and above the plane of view for $\phi_i = \phi_{i+1} = 0$. For the monosubstituted chains, e.g., PVAc, PMA, and PS, the displacements in ϕ_i and ϕ_{i+1} are (+,+) which, as in Figure 5b, increases the distance between O_{i-1} and O_{i+1} or C^{β}_{i-1} and C^{β}_{i+1} from about 2.6 to 3.0 Å. Simultaneously, the distance $H_{i-1}\cdots H_{i+1}$ decreases from 2.62 to 2.39 Å. Similar increase in the $(CH_2)_{i-2}\cdots(CH_2)_{i+2}$ distance and decrease in the $H_{i-1}\cdots H_{i+1}$ distance are also noted for the meso, gg state, in which a (−,−) displacement occurs. The decrease in the H···H distance does not increase the energy significantly. However, in the case of the disubstituted chain, in which H is replaced by CH_3, such a decrease would increase the energy of the $(CH_3)_{i-1}\cdots(CH_3)_{i+1}$ interaction drastically. This is manifested in the energy maps for the meso dyads of PMMA and PMS. In order to substantially relieve both R···R and $CH_3\cdots CH_3$ overlaps simultaneously, the (+,−) or (−,+) displacement is preferred. This situation is shown in Figure 5c, in which the bonds are disposed more like a "parallelogram" rather than as a "rectangle" as in Figure 5a.

For the meso, tt state of PVAc, the energy of a (−,+) or (+,−) displacement, although not lower than that of a (+,+) displacement, is not prohibitively high. For (ϕ_i,ϕ_{i+1}) = (20°,−20°), for example, the distances $O_{i-1}\cdots O_{i+1}$, $C^*_{i-1}\cdots C^*_{i+1}$, and $(CH_3)_{i-1}\cdots(CH_3)_{i+1}$ increase to 2.79, 3.13, and 3.66 Å, respectively, from the values given before for (0°,0°). However, the distances $C^*_{i-1}\cdots O_{i+1}$ = 2.96 Å and $O^c_{i-1}\cdots C^*_{i+1}$ = 3.02 Å at (0°,0°) decrease to 2.74 and 2.66 Å, respectively, for (20°,−20°).

The (−,−) displacement is unfavorable for the meso, tt state of PVAc, since it reverses the situation in Figure 5b, and the distance between R_{i-1} and R_{i+1} decreases. For (−20°,−20°), for example, the distance $(CH_3)_{i-1}\cdots(CH_3)_{i+1}$ is 2.26 Å, which leads to prohibitively high energy.

A (−,+) or (+,−) displacement is noted for the gt (or tg) state of the meso dyad. Here, the interactions are $H_{i-1}\cdots R_{i+1}$ and $(CH_2)_{i-2}\cdots H_{i+1}$. For (120°,0°), the distances $(CH_2)_{i-2}\cdots C^{\alpha}_{i+1}$, $(CH_2)_{i-2}\cdots H_{i+1}$, and $(CH_2)_{i-2}\cdots O^c_{i+1}$ are 3.02, 2.66, and 3.27 Å, respectively, and these increase to 3.18, 2.83, and 3.67 Å for (105°,5°). On the other hand, for a (+,+) displacement, e.g., for (140°,20°), the diagonal interaction[20] between $(CH_2)_{i-2}$ and R_{i+1} becomes predominant. The distances $(CH_2)_{i-2}\cdots C^*_{i+1}$ and $(CH_2)_{i-2}\cdots O^c_{i+1}$ are 3.02 and 3.27 Å at (120°,0°) and these decrease to 2.83 and 3.09 Å for (140°,20°).

Analysis of the interactions and signs of displacements in each of the minima for the meso and racemic dyads shows that, generally, the presence of a diagonal interaction involving nonhydrogen atoms or groups results in a (−,+) or (+,−) displacement. In the absence of such an interaction, displacements of the same sign are observed.

The average energy $\langle E \rangle$, the partition function z, and the average rotation angles were evaluated for each state s using energies calculated at intervals of 5° in ϕ_i and ϕ_{i+1}. These are given by

$$z_s = \sum_{\phi_i} \sum_{\phi_{i+1}} \exp(-E_k/RT) \tag{4}$$

$$\langle E \rangle_s = z_s^{-1} \sum_{\phi_i} \sum_{\phi_{i+1}} \mathrm{E_k} \exp(-E_k/RT) \tag{5}$$

$$\langle \phi_j \rangle_s = z_s^{-1} \sum_{\phi_i} \sum_{\phi_{i+1}} \phi_j \exp(-E_k/RT) \tag{6}$$

where the subscript k refers to each conformation (ϕ_i,ϕ_{i+1}) and $j = i$ or $i + 1$. The results are given in Table III for a temperature of 300 K, with $\sigma = \infty$, 5 Å, and $r_i + r_j + 0.2$. It is seen that although the average energies and the partition functions differ for the various values of σ, the location of the minima is affected very little. The meso, tt state is slightly lower in energy than meso, gt for $\sigma = \infty$. However, with σ = 5 Å and $\sigma = r_i + r_j + 0.2$, the gt state becomes more favorable. This parallels the results on PMA and PS.

Statistical Weights

The energy calculations described above include all the first-order as well as the second-order interactions which depend on the rotations about the bond pair $i, i+1$ within a dyad, i.e., between two C^α atoms. In such a case, it is advantageous to rewrite the matrices $\mathbf{U''}_m$ and $\mathbf{U''}_r$ given in eq 2 and 3 so as to include the first-order interactions.[10] This allows a straightforward evaluation of the statistical weight parameters from the energy calculations. In this rendition, after normalizing with respect to the racemic, tt state,

$$\mathbf{U''}_m = \begin{bmatrix} \omega'' & 1/\eta & \tau\omega'/\eta \\ 1/\eta & \omega/\eta^2 & \tau\omega'/\eta^2 \\ \tau\omega'/\eta & \tau\omega'/\eta^2 & \tau^2\omega\omega''/\eta^2 \end{bmatrix} \tag{7}$$

and

$$\mathbf{U''}_r = \begin{bmatrix} 1 & \omega'/\eta & \tau\omega''/\eta \\ \omega'/\eta & 1/\eta^2 & \tau\omega/\eta^2 \\ \tau\omega''/\eta & \tau\omega/\eta^2 & \tau^2\omega'^2/\eta^2 \end{bmatrix} \tag{8}$$

Not included in $\mathbf{U''}_m$ and $\mathbf{U''}_r$ above are the second-order interactions which depend on the rotations about the bond pair $i-1,i$, flanking the C^α atom. These should now be included in the matrix $\mathbf{U'}$. Thus,

$$\mathbf{U'} = \begin{bmatrix} 1 & 1 & 1 \\ 1 & 0 & 1 \\ 1 & 1 & 0 \end{bmatrix} \tag{9}$$

With the presence of the $\bar{g}$ state, there are five statistical weight parameters to evaluate. The energy corresponding to each of the parameters can be determined by combining the elements of each state of the statistical weight matrices $\mathbf{U''}_m$ and $\mathbf{U''}_r$ and the average energies $\langle E \rangle$ given in Table III for the respective state. A suitable procedure has been described by Suter and Flory.[1] Any one of the statistical weight parameters is denoted by ξ. As in eq 4–6, let s denote any state of the dyad. The energy E_ξ, corresponding to the parameter ξ, is determined from the overdetermined set of 11 linear equations

$$\sum E_\xi - \langle E \rangle_s = 0 \tag{10}$$

The 11 equations correspond to all the nonequivalent states of the meso and racemic dyads, with the exclusion of the racemic, tt state which has a weight of one. Taking the parameters in the order ω'', ω', ω, η, and τ, eq 10, on elaboration, is of the form

$$\left.\begin{aligned} E_{\omega''} + 0 + 0 + 0 + 0 &= \langle E \rangle_{\mathrm{tt},m} \\ 0 + 0 + 0 - E_\eta + 0 &= \langle E \rangle_{\mathrm{tg},m} \\ 0 + E_{\omega'} + 0 - E_\eta + E_\tau &= \langle E \rangle_{\mathrm{t\bar{g}},m} \\ &\cdots \\ &\vdots \\ 0 + 2E_{\omega'} + 0 - 2E_\eta + 2E_\tau &= \langle E \rangle_{\bar{g}\bar{g},r} \end{aligned}\right\} \tag{11}$$

The above set of equations is then solved for the five unknowns.

Introducing the parameter ξ_0, which depends on the effective size of the domains in the energy map,[1]

$$\xi = \xi_0 \exp(-E_\xi/RT) \tag{12}$$

The values of ξ_0, corresponding to the five statistical weight parameters, are determined from the set of 11 linear equations

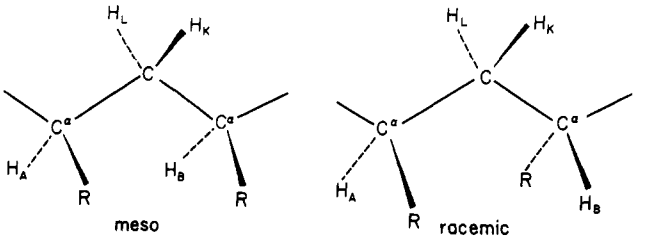

Figure 6. Designation of methine and methylene protons in meso and racemic dyads.

Table IV
Energies Associated with Statistical Weight Parameters and Preexponential Factors

Parameter	$\sigma = \infty$	$\sigma = 5$ Å	$\sigma = r_i + r_j + 0.2$ Å
$E_{\omega''}$	1.229	1.309	1.300
$E_{\omega'}$	0.998	0.873	1.016
E_ω	1.734	1.815	2.009
E_η	−1.441	−1.215	−0.566
E_τ	0.407	0.578	0.735
ω_0''	1.539	1.559	1.771
ω_0'	1.251	1.189	1.354
ω_0	1.555	1.633	1.843
η_0	0.812	0.831	0.841
τ_0	0.498	0.506	0.472

$$\sum \ln \xi_0 - \ln Z_s - (\sum E_\xi/RT) = 0 \tag{13}$$

The values of the parameters thus obtained are given in Table IV for the three values of σ used here. It is seen that significant variation in energy is noted for E_η, which parallels the result for the meso, gt state given in Table III. The preexponential factors η_0, ω_0, etc., show insignificant variation with σ. The value of $E_{\omega''}$ (which represents R···R interaction) in this case is lower than that for polystyrene and is of the same order of magnitude as for PMA. In spite of the size and branching of the side group in PVAc, the values of E_τ and τ_0 calculated here are similar to the values of $E_\tau = 500$ cal mol^{-1} and $\tau_0 = 0.4$ deduced for polypropylene.[1]

Calculation of NMR Coupling Constants

In addition to being a useful tool for the determination of tacticities, NMR spectral data have been applied to deduce the preferred conformations of dyads and triads of vinyl polymers.[3,21-26] The vicinal coupling between the methine proton and the methylene protons depends on the conformation of the skeletal bond. The observed coupling constant is an average over the preferred conformations of the bond. Following the terminology of the previous authors,[21-26] the methine and methylene protons are labeled as in Figure 6. In the meso dyad, K is anti to both A and B (syn to R) and L is syn to both A and B. For the racemic isomer, K is anti to A and syn to B, L is syn to A and anti to B. Two protons are syn if they lie on the same side and anti if on opposite sides of the plane of the skeletal bonds when the latter are in the trans planar conformation. Due to the symmetry inherent in the dyads, the following relations exist between the averaged coupling constants:

$$\left.\begin{aligned} \langle J_{AK} \rangle &= \langle J_{BK} \rangle = \langle J_{syn} \rangle \\ \langle J_{AL} \rangle &= \langle J_{BL} \rangle = \langle J_{anti} \rangle \end{aligned}\right\} \text{meso} \tag{14}$$

$$\left.\begin{aligned} \langle J_{AL} \rangle &= \langle J_{BK} \rangle = \langle J_{syn} \rangle \\ \langle J_{AK} \rangle &= \langle J_{BL} \rangle = \langle J_{anti} \rangle \end{aligned}\right\} \text{racemic} \tag{15}$$

The difference between $\langle J_{anti} \rangle$ and $\langle J_{syn} \rangle$ can be calculated theoretically and compared with experimental results. These average coupling constants can be written in terms of the

probabilities of the t, g, and $\bar{g}$ conformations of the skeletal bond. Thus,

$$\langle J_{AK} \rangle = p_t J_t + p_g J_g + p_{\bar{g}} J_g \quad (16)$$

$$\langle J_{AL} \rangle = p_t J_g + p_g J_t + p_{\bar{g}} J_g \quad (17)$$

Here, J_t and J_g are the trans and gauche coupling constants representing the dihedral angle between the protons A and K or A and L in the t, g, or $\bar{g}$ states. It follows from eqs 16 and 17 that

$$\Delta J = \langle J_{AK} \rangle - \langle J_{AL} \rangle = (J_t - J_g)(p_t - p_g) \quad (18)$$

or

$$\Delta J = \delta J(p_t - p_g) \quad (19)$$

In the case where the $\bar{g}$ state is deleted, $p_g = 1 - p_t$ and eq 19 reduces to

$$\Delta J = \delta J(2p_t - 1) \quad (20)$$

which is the equation used by Yoon et al.[3] for PMA.

In the following calculations eq 19 was used. The a priori probability p_s (s = t or g) for a bond i was calculated according to

$$p_{s,i} = Z^{-1}\mathbf{U}_0 \left[\prod_{h=2}^{i-1} \mathbf{U}_h\right] \left[\hat{\mathbf{U}}_{s,i}\right] \left[\prod_{j=i+1}^{x-1} \mathbf{U}_j\right] \mathbf{U}_x \quad (21)$$

where $\hat{\mathbf{U}}_{s,i}$ is the matrix obtained from the statistical weight matrix $\mathbf{U}_i$ for the bond i by replacing all elements with zero, except those in column s. The configurational partition function Z is defined by

$$Z = \mathbf{U}_0 \left[\prod_{k=1}^{x-1} \mathbf{U}'_k \mathbf{U}''_k\right] \mathbf{U}_x \quad (22)$$

and

$$\mathbf{U}_0 = [1 \quad 0 \quad 0], \qquad \mathbf{U}_x = \begin{bmatrix} 1 \\ 1 \\ 1 \end{bmatrix} \quad (23)$$

The product $\mathbf{U}'_k \mathbf{U}''_k$ refers to the kth dyad and reflects its stereochemical character, either meso or racemic. For meso and racemic dyads, eq 21 reduces to

$$p_{s,m} = Z^{-1}(\mathbf{U}_0 \mathbf{U}' \hat{\mathbf{U}}_{s,m} \mathbf{U}_x) \quad (24)$$

and

$$p_{s,r} = Z^{-1}(\mathbf{U}_0 \mathbf{U}' \hat{\mathbf{U}}_{s,r} \mathbf{U}_x) \quad (25)$$

For the isotactic triad, the probability is taken as an average of p and p' given by

$$p_{s,\text{iso}} = Z^{-1}(\mathbf{U}_0 \hat{\mathbf{U}}' \mathbf{U}''_m \mathbf{U}' \mathbf{U}''_m \mathbf{U}_x) \quad (26)$$

and

$$p'_{s,\text{iso}} = Z^{-1}(\mathbf{U}_0 \mathbf{U}' \hat{\mathbf{U}}''_m \mathbf{U}' \mathbf{U}''_m \mathbf{U}_x) \quad (27)$$

The expressions for the syndiotactic triad are similar, with the first $\mathbf{U}''_m$ in eq 26 and 27 being replaced by $\mathbf{U}''_r$.

The expression for the a priori probability given in eq 21 is applicable to chains of any length. Moritani and Fujiwara[26] have given analytical expressions using statistical weight parameters to calculate ΔJ for meso and racemic dyads. Their equations are simply a combination of eq 22 and 24 or 25 after the multiplication of the matrices. Extension of the equations of Moritani and Fujiwara for triads, tetrads etc., becomes lengthy and complicated. In this respect, the rendition of the expression in terms of matrices is most effective.

The values of ΔJ calculated for the meso and racemic dyads and triads of PVAc are given in Figures 7 and 8 for various values of $E_{\omega''}$ and E_η. The values of $(\Delta J)_m$ and $(\Delta J)_{mm}$ decrease significantly with an increase of $E_{\omega''}$ and E_η. For a chosen value of τ, ω', η, and ω, an increase in $E_{\omega''}$ decreases the population of the trans and hence the values of p_t and ΔJ. A change in $E_{\omega''}$ has very little influence on the values of $(\Delta J)_r$ and $(\Delta J)_{rm}$.

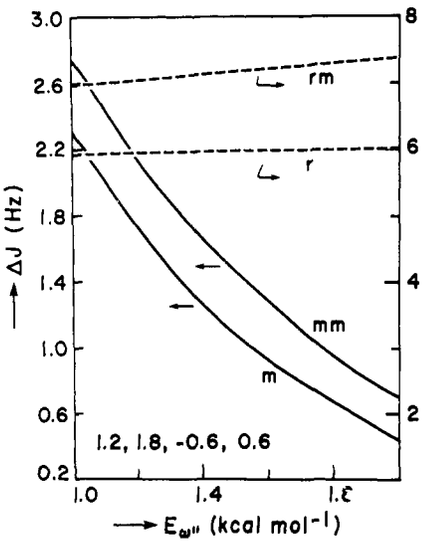

Figure 7. Variation of ΔJ for meso and racemic, dyads and triads of PVAc, with $E_{\omega''}$. The values of $E_{\omega'}$, E_ω, E_η, and E_τ, in that order, are marked.

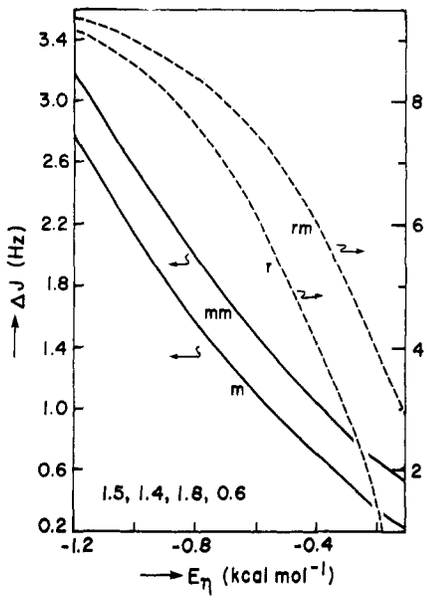

Figure 8. Variation of ΔJ for meso and racemic dyads and triads of PVAc, with E_η. The values of $E_{\omega''}$, $E_{\omega'}$, E_ω, and E_τ, in that order, are marked.

The values of ΔJ for all four cases show significant variation with E_η. For both meso and racemic dyads, the g state depends inversely on η. Thus p_g increases with E_η and reduces the value of ΔJ.

Experimental values of ΔJ for isotactic and syndiotactic isomers of the acetate derivatives of 2,4-pentanediol and 2,4,6-heptanetriol were determined by Fujiwara et al.[24] and Doskočilová et al.[25] These are 0.8, 1.1, 6.5, and 6.8 Hz for $(\Delta J)_m$, $(\Delta J)_{mm}$, $(\Delta J)_r$, and $(\Delta J)_{rm}$, respectively. Figures 7 and 8 show that these values are reproduced by $E_{\omega''} \approx 1.7$ and $E_\eta \approx -0.5$ kcal mol^{-1}.

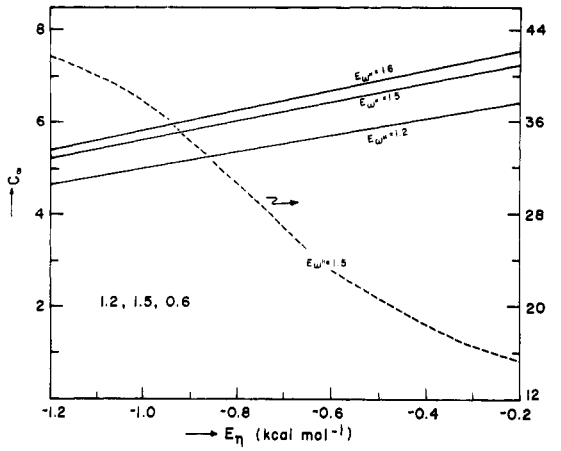

Figure 9. Variation of C_∞ with E_η for isotactic (solid lines, left ordinate) and syndiotactic (dashed line, right ordinate) PVAc. The values of $E_{\omega''}$ are marked and those of $E_{\omega'}$, E_ω, and E_τ, in that order, are given.

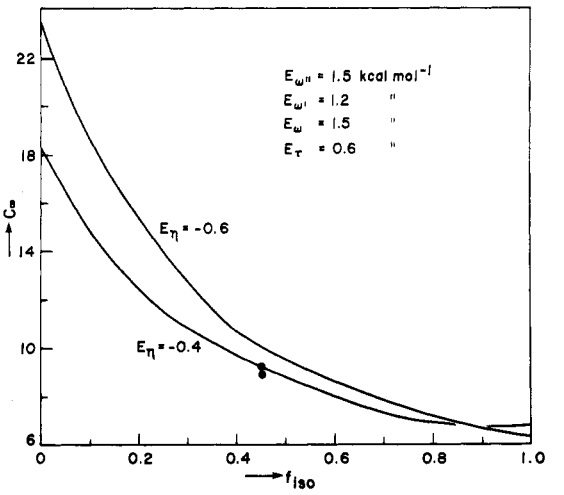

Figure 10. Variation of C_∞ as a function of the tacticity of PVAc. The experimental values are shown[27,28] by the solid circles.

Characteristic Ratios

The characteristic ratios $C_\eta = \langle r^2\rangle_0/nl^2$ were calculated using the matrix formulation which includes the calculated average locations of the pair of bonds in a dyad.[2,6] The end-to-end distance is given by

$$\langle r^2\rangle_0 = Z^{-1}\mathcal{G}_0\left(\prod_{k=1}^{x-1}\mathcal{U}'\mathcal{G}_k\right)\mathcal{G}_x \qquad (28)$$

where Z is calculated according to eq 22 and $\mathcal{U}' = \mathbf{U}' \times \mathbf{E}_5$, in which $\mathbf{E}_5$ is the identity matrix of order five. The generator matrices $\mathcal{G}_i$ take the form given before.[2,6]

The characteristic ratios calculated for isotactic and syndiotactic chains with various values of $E_{\omega''}$ and E_η are shown in Figure 9. For isotactic PVAc, the value of C_∞ increases with $E_{\omega''}$ which is similar to the results obtained for PS and PMA. The increase in $E_{\omega''}$ decreases the population of the tt state relative to the gt (or tg) state. The perpetuation of the latter promotes a sequence of 3_1 helices. The same phenomenon leads to an increase of C_∞ with E_η. Since the gt (or tg) state depends inversely on η, their frequency of occurrence increases with E_η.

For the syndiotactic chain, the characteristic ratio decreases with an increase in E_η. This also parallels the results on PS and with an increase in E_η. This also parallels the results on PS and PMA. Although the gt conformation of both iso- and syndiotactic chains depends inversely on η, the C_∞ varies differently with η in these cases. This is necessarily due to the statistical weights associated with the tt state of the meso and racemic dyads. In the former, the preference for the gt state is large. The occurrence of tt state serves to disrupt the helical sequence generated by the gt state. An increase in E_η increases the relative population of the gt state, the sequence of helical segments, and hence the C_∞. For the racemic dyad, the tt state is more favorable than gt and hence the C_∞ is large when the population of the gt state is negligible, e.g., with $E_\eta = -1.2$ kcal mol^{-1}. The frequency of the gt state increases with E_η and interspersion of the gauche states in an otherwise all-trans chain reduces the value of C_∞ significantly.

The characteristic ratios for Monte Carlo chains, with various amounts of isotactic content, are shown in Figure 10. The high value of C_∞ in the range of predominant syndiotacticity and a drastic reduction for $f_{iso} > 0.2$ seem to be typical of monosubstituted vinyl chains. The convex shape of the curve of C_∞, observed for disubstituted chains, e.g., PMMA and PMS, is absent. For the latter,[4,6] it was shown that the value of C_∞ for the stereoirregular chain is greater than that of either purely isotactic or syndiotactic chain. The experimental values[27,28] of the characteristic ratio of atactic PVAc are marked in Figure 10. It was shown[7,8] that the free radical initiated PVAc is highly atactic, with $f_{iso} = 0.55$. Agreement between the calculated and experimental results is good for $E_\eta = -0.4$ kcal mol^{-1}.

Concluding Remarks

The NMR data and the characteristic ratios are reproduced by $E_{\omega''} \approx 1.5$, $E_\eta \approx -0.5$, $E_{\omega'} \approx 1.2$, $E_\omega \approx 1.5$, and $E_\tau \approx 0.6$ kcal mol^{-1}. These are close to the values deduced from energy calculations. In general, the use of $\sigma = r_i + r_j + 0.2$ in the calculations leads to energy parameters which give good agreement with experimental results. Thus, the use of σ which depends on the type of interacting pair of atoms or groups seems to be pertinent. The conformational features of PVAc differ from those of other vinyl chains bearing planar substituents. The $\bar{g}$ state cannot be ruled out as with the other chains.

Acknowledgments. The author thanks Dr. M. L. Hair of this research center for his interest in this work and the encouragement he provided.

References and Notes

(1) U. W. Suter and P. J. Flory, *Macromolecules*, **8**, 765 (1975).
(2) D. Y. Yoon, P. R. Sundararajan, and P. J. Flory, *Macromolecules*, **8**, 776 (1975).
(3) D. Y. Yoon, U. W. Suter, P. R. Sundararajan, and P. F. Flory, *Macromolecules*, **8**, 784 (1975).
(4) P. R. Sundararajan and P. J. Flory, *J. Am. Chem. Soc.*, **96**, 5025 (1974).
(5) P. R. Sundararajan, *J. Polym. Sci., Polym. Lett. Ed.*, **15**, 699 (1977).
(6) P. R. Sundararajan, *Macromolecules*, **10**, 623 (1977).
(7) F. A. Bovey, E. W. Anderson, D. C. Douglass, and J. A. Manson, *J. Chem. Phys.*, **39**, 1199 (1963).
(8) K. Fujii, *Macromol. Rev.*, **5**, 431 (1971).
(9) P. J. Flory, "Statistical Mechanics of Chain Molecules", Interscience, New York, N.Y., 1969, Chapter VI.
(10) P. J. Flory, P. R. Sundararajan, and L. C. DeBolt, *J. Am. Chem. Soc.*, **96**, 5015 (1974).
(11) See ref 9, p 50.
(12) G. Nemethy and H. A. Scheraga, *Biopolymers*, **3**, 155 (1965).
(13) A. Sarko and R. H. Marchessault, *J. Am. Chem. Soc.*, **89**, 6454 (1967).
(14) S. M. Gabbay, P. R. Sundararajan, and R. H. Marchessault, *Biopolymers*, **11**, 79 (1972); P. R. Sundararajan and R. H. Marchessault, *Biopolymers*, **11**, 829 (1972).
(15) D. A. Brant, W. G. Miller, and P. J. Flory, *J. Mol. Biol.*, **23**, 47 (1967).
(16) C. P. Smyth, "Dielectric Behaviour and Structure", McGraw-Hill, New York, N.Y., 1955, p 244.
(17) D. Y. Yoon and P. J. Flory, *Polymer*, **16**, 645 (1975).
(18) D. Y. Yoon and P. J. Flory, *Macromolecules*, **9**, 299 (1976).
(19) T. Bleha and L. Valko, *Polymer*, **17**, 298 (1976).
(20) The diagonal interactions[4,6] are those between groups attached to C^α_{i-1} and C^α_{i+1} and which are on opposite sides of the plane defined by the skeletal bonds i, $i+1$. For example, in Figure 1, the interaction between H_{i-1} and R_{i+1} or R_{i-1} and H_{i+1} is a diagonal interaction.
(21) D. Doskočilová, S. Sýkora, H. Pivcová, B. Obereigner, and D. Lim, *J.*

Polym. Sci., Part C, **23**, 365 (1968).
(22) F. A. Bovey, F. P. Hood, E. W. Anderson, and L. C. Snyder, *J. Chem. Phys.*, **42**, 3900 (1965).
(23) T. Yoshino, Y. Kikuchi, and J. Komiyama, *J. Phys. Chem.*, **70**, 1059 (1966).
(24) Y. Fujiwara, S. Fujiwara, and K. Fujii, *J. Polym. Sci., Part A-1*, **4**, 257 (1966).
(25) D. Doskočilová, J. Štokr, E. Votavova, B. Schneider, and D. Lim, *J. Polym. Sci., Part C*, **16**, 2225 (1967).
(26) T. Moritani and Y. Fujiwara, *J. Chem. Phys.*, **59**, 1175 (1973).
(27) A. R. Schultz, *J. Am. Chem. Soc.*, **76**, 3422 (1954).
(28) M. Matsumoto and Y. Ohyanagi, *J. Polym. Sci.*, **50**, S1 (1961).
(29) I. Sakurada and K. Fuchino, *Sci. Pap. Inst. Phys. Chem. Res. (Jpn.)*, **39**, 78 (1941); cited in ref 8, p 450.
(30) W. J. Dulmage, *J. Polym. Sci.*, **26**, 277 (1957).
(31) H. Chanzy and E. Roche, *J. Polym. Sci., Polym. Phys. Ed.*, **12**, 2583 (1974); **13**, 1859 (1975).
(32) E. Roche, H. Chanzy, M. Boudeulle, R. H. Marchessault, and P. R. Sundararajan, *Macromolecules*, submitted.
(33) A. Sarko and R. H. Marchessault, *Science*, **154**, 3757 (1966).
(34) R. H. Marchessault and P. R. Sundararajan, *Pure Appl. Chem.*, **42**, 399 (1975).

Hypersonic Relaxation and the Glass–Rubber Relaxation in Poly(propylene glycol)

G. D. Patterson,* D. C. Douglass, and J. P. Latham

Bell Laboratories, Murray Hill, New Jersey 07974. *Received April 26, 1977*

ABSTRACT: Hypersonic relaxation in poly(propylene glycol) (PPG) was studied using Brillouin spectroscopy. The loss tan δ exhibited two maxima as a function of temperature. The higher temperature maximum at 100 °C agreed with recent[1] dielectric relaxation results on PPG at gigahertz frequencies. The secondary maximum at 50 °C agreed with previous hypersonic relaxation studies of PPG and fell on an extrapolation of the secondary glass–rubber relaxation data. NMR relaxation was also studied on the same sample. The T_1 minimum occurred at 270 K and the $T_{1\rho}$ minimum at 235 K. These results agreed with dielectric relaxation in the megahertz and kilohertz regions. No secondary glass–rubber relaxation was observed by NMR, but the rotation of methyl groups was detected.

Dielectric relaxation in poly(propylene glycol) (PPG) has been examined from just greater than 10^{-4} Hz to just less than 10^{10} Hz.[1-3] The loss maxima for the primary glass–rubber relaxation could be correlated[1] over the entire frequency range with an equation of the form

$$\log f = \log f_\infty - \frac{B}{T - T_0} \tag{1}$$

where f_∞ is the extrapolated frequency at infinite temperature and T_0 is a temperature below the nominal T_g. In addition to the primary loss peak McCammon and Work[4] reported a weak secondary peak in the dielectric loss spectrum. The secondary relaxation has also been studied by dynamic mechanical methods.[5,6] The secondary main chain glass–rubber relaxation data can be correlated according to

$$\log f = \log f_\infty - \frac{B}{T} \tag{2}$$

Recent studies[7-9] of hypersonic relaxation in polymers using Brillouin spectroscopy have revealed that the temperatures of maximum loss determined by this technique agree with an extrapolation of the lower frequency secondary relaxation data according to eq 2. In most polymers the primary and secondary main chain glass–rubber relaxations are not resolved at 10^9 Hz. Thus, only a single loss peak is observed by Brillouin scattering or dielectric relaxation at hypersonic frequencies. However, the temperature of maximum loss for PPG determined by Yano et al.[1] using dielectric relaxation is higher than the hypersonic results reported by Wang and Huang[10] and Lindsay et al.[11] The dielectric relaxation results[1] fit the extrapolated primary relaxation line. The observed hypersonic relaxation falls on a reasonable extrapolation of the limited secondary relaxation data.[4-6]

There is no reason to expect that hypersonic relaxation would be sensitive only to the secondary relaxation process in a region where the two relaxations could be resolved. However, the magnitude of tan δ at the two temperatures of maximum loss could be quite different. The failure of Yano et al.[1] to detect the secondary relaxation at gigahertz frequencies can easily be attributed to the very small dielectric loss associated with this process.

In the present work we reexamine hypersonic relaxation in poly(propylene glycol) using Brillouin spectroscopy. In addition, new data were obtained from nuclear magnetic relaxation (NMR) for PPG.

Experimental Section

Materials. Poly(propylene glycol) of nominal molecular weight 4000 was obtained from Polysciences, Inc. It is important to choose the molecular weight to be high enough to obtain the limiting results for both the primary and secondary main-chain glass–rubber relaxations.[8] The fluid was filtered directly into a 1-cm square quartz fluorimeter cell for the Brillouin scattering experiments or into a 5-mm NMR tube for the nuclear magnetic relaxation experiments.

Brillouin Scattering. Brillouin spectra were obtained as described previously.[7-9] The incident wavelength was 5145 Å and the scattering angle was 90°. The free spectral range of the Fabry–Perot interferometer was 19.3 GHz. The spectra were recorded digitally with two orders in 1024 points. The observed Brillouin spectra were deconvoluted by comparing them with spectra calculated by convoluting the true instrumental function with the theoretical form for the Brillouin spectrum. For our interferometer this procedure resulted in subtracting the instrumental half-width at half-height from the observed Brillouin line widths since the transmission function was accurately given by an Airy function. Measurements of the Rayleigh–Brillouin spectrum were carried out from −10 to 170 °C. The loss tan δ was calculated according to

$$\tan \delta = (2\Gamma_l/\Delta\omega_l)(1 - (\Gamma_l/\Delta\omega_l)^2)^{-1} \tag{3}$$

The NMR data reported are obtained from longitudinal relaxation in the laboratory, T_1, and rotating frames, $T_{1\rho}$, by conventional 180–90° and spin-locking pulse sequencies, respectively.[12]

Results and Discussion

The Brillouin splittings $\Delta\omega_l$ and line widths Γ_l are listed as a function of temperature in Table I. The frequencies and tan δ are plotted vs. T in Figure 1. The loss maximum at approximately 50 °C and 5.43 GHz is in good agreement with the previous results of Wang and Huang[10] and Lindsay et al.[11] In

0024-9297/78/2211-0263$01.00/0